

Cobalt–Oxo Core of a Water-Oxidizing Catalyst Film

M. Risch, V. Khare, I. Zaharieva, L. Gerencser, P. Chernev, and H. Dau*

Freie Universität Berlin, FB Physik, Arminiallee 14, 14195 Berlin, Germany

Received March 18, 2009; E-mail: holger.dau@physik.fu-berlin.de

Photosynthetic water oxidation is crucial for life on Earth. It is efficiently catalyzed by a pentanuclear Mn_4Ca complex bound to amino acid residues of photosystem II (PSII), which is characterized by a compact metal–oxo core with several di- μ -oxo bridges between Mn ions.^{1–4} For large-scale technological production of molecular hydrogen (or other fuels) from water, synthetic water-oxidation catalysts that are (i) similarly efficient as the photosynthetic Mn complex and (ii) based on inexpensive and abundant materials are needed.

Recently, several new transition-metal complexes for homogeneous catalysis of water oxidation have been described; typically, rare metals have been employed.^{5,6} A cobalt catalyst for electrochemical water oxidation reported by Kanan and Nocera⁷ has attracted much interest because of its efficiency at neutral pH and self-assembly from low-cost materials. This catalyst assembles as an amorphous layer on inert cathodes by electrodeposition starting from an aqueous solution of simple cobalt and phosphate salts. The resulting cobalt catalyst film (CoCF) also contains phosphate and potassium, at an approximate Co/P/K stoichiometry of 2–3:1:1.⁷ Its self-assembly and repair mechanisms bear interesting similarities to the formation of the Mn complex that facilitates water oxidation in PSII. To elucidate the Co oxidation state, the coordination environment, and the dominating structural motifs of the amorphous CoCF, we employed X-ray absorption spectroscopy (XAS).^{8–10}

The film was formed by cathodic electrodeposition from an aqueous solution of KH_2PO_4 and K_2HPO_4 (pH 7) containing $Co(OH_2)_6(NO_3)_2$, with concentrations of 0.1 M (KPi) and 0.5 mM (Co^{2+}). The cathode material was indium tin oxide (ITO) deposited on glass; a voltage of 1.4 V (vs NHE) was applied. XAS samples were prepared in six different ways [see the Supporting Information (SI)]; the following procedure was used for the spectra shown in Figures 1 and 2: After 70 min of film formation (paralleled by water oxidation), the CoCF-covered cathode was rapidly disconnected and removed from solution. This was followed by fast freezing of the still-wet electrode in liquid nitrogen and X-ray measurements at 20 K (quasi-in situ sample). Fluorescence-detected XAS spectra at the Co K-edge were collected at the KMC-1 beamline at BESSY (Berlin). For comparison, spectra of microcrystalline powders of $[Co^{II}(OH_2)_6](NO_3)_2$ and $[Co^{III}(NH_3)_6]Cl_3$ were also collected.

Figure 1 shows the X-ray absorption near-edge structure (XANES) spectrum of a quasi-in situ sample obtained by direct freezing of a wet CoCF electrode. The edge position of CoCF (7717.5 ± 0.2 eV at half-height of the normalized edge-jump) is identical to that of the Co^{III} standard and 3 eV higher than that of the Co^{II} compound, suggesting a mean Co oxidation state of $3+$ in the CoCF. The shape of the XANES spectrum reflects the ligand type and coordination geometry of the X-ray-absorbing transition metal. In comparison with the spectrum of the Co^{II} compound, the CoCF spectrum is shifted to higher energies but is otherwise very similar. This suggests near-octahedral Co coordination by six oxygen ligands (a prevalence of O_h Co^{III}).

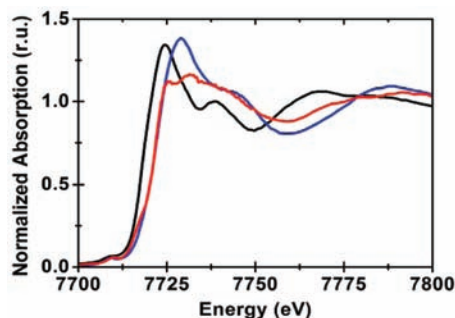


Figure 1. K-edge XANES spectra of CoCF (blue), $[Co^{II}(OH_2)_6](NO_3)_2$ (black), and $[Co^{III}(NH_3)_6]Cl_3$ (red).

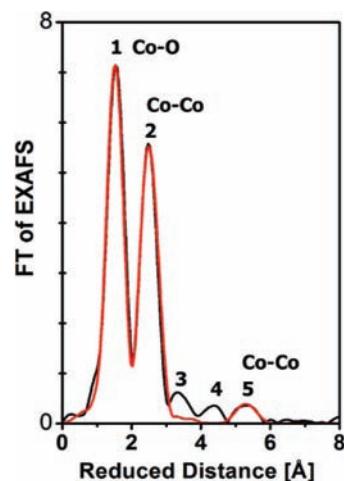


Figure 2. FT of an EXAFS spectrum of the Co catalyst (black line, experimental spectrum; red line, EXAFS simulation). The indicated reduced distances were obtained directly by Fourier transformation; the internuclear distances determined by EXAFS simulations are ~ 0.3 Å longer. For Fourier transformation of the k^3 -weighted EXAFS oscillations, a \cos^2 window function covering the complete k range (2 – 14 \AA^{-1}) was used, thereby ensuring complete suppression of sidelobe artifacts.

The XANES and extended X-ray absorption fine structure (EXAFS) spectra of the Co catalyst were similar for the quasi-in situ condition, dried CoCF on ITO electrodes, and dried CoCF ground to a powder, regardless of the details of the preparation method (Figure S1 in the SI). We therefore conclude that the CoCF is surprisingly robust against dehydration, air exposure, and mechanical treatment.

Figure 2 shows the Fourier transform (FT) of an EXAFS spectrum of the CoCF. Ligation of Co by ~ 6 oxygens at a distance of 1.89 Å was determined by EXAFS simulations (Table 1), confirming the prevalence of $Co^{III}O_6$ in the catalyst. A prominent Co–Co distance of 2.81 Å accounts for ~ 4 metal–metal interactions per Co ion. Distances close to 2.8 Å are typical for Co atoms connected by di- μ -oxo bridges, specifically in Co–oxo cubanes.^{11,12}

Table 1. Parameters for the EXAFS Simulation in Figure 2^a

| peak no. | atoms | <i>N</i> | <i>R</i> (Å) | σ (Å) |
|----------|---------|----------|--------------|--------------|
| 1 | Co–O | 5.8 | 1.89 | 0.051 |
| | min/max | 5.2/6.2 | 1.88/1.90 | 0.043/0.056 |
| 2 | Co–Co | 4.0 | 2.81 | 0.069 |
| | min/max | 3.1/6.1 | 2.79/2.82 | 0.057/0.088 |
| 5 | Co–Co | 0.9 | 5.62 | 0.067* |
| | min/max | 0.6/1.0 | 5.61/5.65 | |

^aThe parameter marked by an asterisk was fixed, and all of the other parameters were determined by curve-fitting of the data (*k* range 3–12 Å⁻¹). The EXAFS coordination, *N*, represents the number of backscattering atoms per absorbing cobalt at a distance close to *R*. In the rows labeled “min/max”, error range estimates are provided. For further details, see the SI.

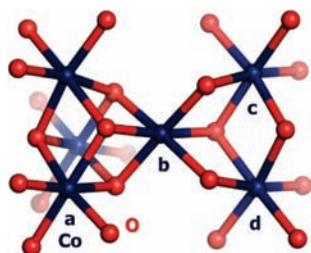


Figure 3. Proposed structural motif deduced from XAS data relating to the bulk of the CoCF (cobalt in blue, oxygen in red).

The *N* value (>3) indeed implies the presence of interconnected incomplete or complete cubane units [Co_{3/4}(μ-O)₄; see Figure 3].

The FT peak 5 can be assigned to a Co–Co distance of 5.62 Å, which can be explained by two cubanes sharing a Co corner (the *a*–*c* distance in Figure 3). The small amplitude of the respective FT peak likely results from a low number of Co–Co vectors (<1 per Co atom), as suggested by multiple-scattering EXAFS simulations. In layer-forming metal dioxides (e.g., MnO₂ in acid busenite), there are six metal–metal distances of ~5.6 Å (i.e., 2 × 2.8 Å), resulting in a clearly more sizable FT peak (Figure S6). Thus, rather than an extended CoO₂ structure, the central structural motif of CoCF likely consists of clusters of complete or incomplete Co–oxo cubanes that share Co corners, as shown in Figure 3. The position of peak 4 in Figure 2 is consistent with a Co–Co distance of ~4.8 Å (see Table S2), as predicted for the suggested structure (the *a*–*d* distance in Figure 3).

In PSII membranes deposited in the form of thick films (50–500 μm) on a flat support, a clear linear dichroism in the X-ray spectra is observable because of the unidirectional orientation of the Mn complex with respect to the sample support.^{13,14} We investigated whether a similar dichroism was observable in the CoCF spectra by measuring spectra at various angles between the polarized X-ray beam and the sample surface. The identity of the XANES and EXAFS spectra collected at various angles indicates a fully isotropic distribution of the Co–O and Co–Co vectors in the material. This is predicted for cubane units but also explainable by a lack of macroscopic order in the CoCF.

The XAS data excludes direct Co–P bonds. The presence of phosphorus in the second coordination sphere of Co is not indicated by the data. However, a limited number of phosphorus atoms at ~3 Å (possible Co–P distance in a Co–O–PO₃ motif) could be hidden in the 2.8 Å Co–Co peak (Figure S4). Thus, the phosphate ions present in CoCF could form a (poly)phosphate framework¹⁵ that provides ligands to the Co–oxo units of Figure 3. Without

providing definitive proof, EXAFS simulations furthermore indicate that potassium atoms at a distance of 3.8 Å from Co could contribute to peak 3 (Table S2, Figure S5). Further XAS experiments addressing the coordination of potassium and phosphorus are in preparation.

In summary, the central structural unit found in the bulk of the novel water-oxidation catalyst described by Kanan and Nocera⁷ likely is a cluster of interconnected complete or incomplete Co^{III}–oxo cubanes. Phosphate oxygens as Co-bridging ligands can be excluded (this would cause elongation of the Co–Co distance beyond 2.81 Å), but terminal phosphate ligation is conceivable. Potassium ligation to three Co-bridging oxygens could result in Co₃K(μ-O)₄ cubanes, in analogy to the Mn₃Ca(μ-O)₄ cubane motif proposed for the photosynthetic Mn complex.^{3,16,17}

The similarities in function and oxidative self-assembly of the CoCF and the catalytic Mn complex in photosynthesis are striking.^{1,2,18,19} Our study establishes a close analogy also with respect to the metal–oxo core of the catalyst. Further studies are required to address in more detail the structure–function relations in the biological and the artificial water-oxidation catalysts.

Acknowledgment. We thank S. Wasle, B. Pettinger, G. Wagner, and M. Wolf (Fritz-Haber Institute, Berlin) for their contributions to complementary experiments. We thank F. Schäfers and M. Mertin (beamline KMC-1, BESSY, Berlin) for excellent technical support and M. Haumann (FU Berlin) for valuable discussions. Financial support by the UniCat cluster of excellence (Unifying Concepts in Catalysis, Berlin) and the European Union (SOLAR-H2, 212508) is gratefully acknowledged.

Supporting Information Available: Further experimental details, XANES spectra for various preparation procedures, details of EXAFS simulations, and comparison of the spectra of the CoCF and a layered manganese dioxide (acid busenite). This material is available free of charge via the Internet at <http://pubs.acs.org>.

References

- McEvoy, J. P.; Brudvig, G. W. *Chem. Rev.* **2006**, *106*, 4455–4483.
- Dau, H.; Haumann, M. *Coord. Chem. Rev.* **2008**, *252*, 273–295.
- Ferreira, K. N.; Iverson, T. M.; Maghlaoui, K.; Barber, J.; Iwata, S. *Science* **2004**, *303*, 1831–1838.
- Yano, J.; Kern, J.; Sauer, K.; Latimer, M. J.; Pushkar, Y.; Biesiadka, J.; Loll, B.; Saenger, W.; Messinger, J.; Zouni, A.; Yachandra, V. K. *Science* **2006**, *314*, 821–825.
- Sala, X.; Romero, I.; Rodríguez, M.; Escriche, L.; Llobet, A. *Angew. Chem., Int. Ed.* **2009**, *48*, 2842–2852.
- Meyer, T. J. *Nature* **2008**, *451*, 778–779.
- Kanan, M. W.; Nocera, D. G. *Science* **2008**, *321*, 1072–1075.
- George, G. N.; Hedman, B.; Hodgson, K. O. *Nat. Struct. Biol.* **1998**, *5*, 645–647.
- Dau, H.; Liebisch, P.; Haumann, M. *Anal. Bioanal. Chem.* **2003**, *376*, 562–583.
- Penner-Hahn, J. E. *Coord. Chem. Rev.* **1999**, *190–192*, 1101–1123.
- Ama, T.; Rashid, M. M.; Yonemura, T.; Kawaguchi, H.; Yasui, T. *Coord. Chem. Rev.* **2000**, *198*, 101–116.
- Dimitrou, K.; Foltling, K.; Streib, W. E.; Christou, G. *J. Am. Chem. Soc.* **1993**, *115*, 6432–6433.
- George, G. N.; Prince, R. C.; Cramer, S. P. *Science* **1989**, *243*, 789–791.
- Dittmer, J.; Dau, H. *J. Phys. Chem. B* **1998**, *102*, 8196–8200.
- Natarajan, S.; Mandal, S. *Angew. Chem., Int. Ed.* **2008**, *47*, 4798–4828.
- Dau, H.; Grundmeier, A.; Loja, P.; Haumann, M. *Philos. Trans. R. Soc. London, Ser. B* **2008**, *363*, 1237–44.
- Sproviero, E. M.; Gascon, J. A.; McEvoy, J. P.; Brudvig, G. W.; Batista, V. S. *J. Am. Chem. Soc.* **2008**, *130*, 6728–6730.
- Kanan, M. W.; Surendranath, Y.; Nocera, D. G. *Chem. Soc. Rev.* **2009**, *38*, 109–114.
- Dasgupta, J.; Ananyev, G. M.; Dismukes, G. C. *Coord. Chem. Rev.* **2008**, *252*, 347–360.

JA902121F